Bioorganic Chemistry 84 (2019) 468–477

Contents lists available at ScienceDirect

Bioorganic Chemistry

journal homepage: www.elsevier.com/locate/bioorg

Design, synthesis and biological evaluation of novel β-pinene-based thiazole derivatives as potential anticancer agents *via* mitochondrial-mediated apoptosis pathway

Yunyun Wang[a], Chenliang Wu[a], Qiangjian Zhang[a], Yu Shan[b], Wen Gu[a,c,*], Shifa Wang[a,c,*]

[a] College of Chemical Engineering, Nanjing Forestry University, Nanjing 210037, PR China
[b] Institute of Botany, Jiangsu Province and Chinese Academy of Sciences (Nanjing Botanical Garden Mem. Sun Yat-Sen), 210014, PR China
[c] Co-Innovation Center of Efficient Processing and Utilization of Forest Resources, Nanjing Forestry University, Nanjing 210037, PR China

ARTICLE INFO

Keywords:
β-Pinene-based thiazole derivatives
Anticancer
Mitochondrial membrane potential
Reactive oxygen species

ABSTRACT

A series of novel β-pinene-based thiazole derivatives were synthesized and characterized by HRMS, ^{1}H NMR, and ^{13}C NMR analyses as potential antineoplastic agents. Derivatives were evaluated for their anticancer activities *in vitro*, and the data manifested that most target compounds showed potent anti-proliferative activities against three human cancer cell lines. Especially, compound **5g** displayed excellent cytotoxic activity against Hela, CT-26, and SMMC-7721 cell lines with IC_{50} values of 3.48 ± 0.14, 8.84 ± 0.16, and 6.69 ± 0.15 μM, respectively. To determine the underlying mechanism of compound **5g** on cell viability, DAPI staining, Annexin-V/PI staining, JC-1 staining, DCFDA staining, and Western blot analysis were performed. Our data showed that compound **5g** inhibited cell proliferation by inducing apoptosis and cell cycle arrest of Hela cells at the G0/G1 phase in a dose dependent manner. Further studies revealed that compound **5g** enhanced levels of reactive oxygen species (ROS), caused a decrease in mitochondrial membrane potential, increased the release of mitochondrial cytochrome *C*, and affected the expression of Bax, Bcl-2, caspase-3 and caspase-9. Thus, our findings indicated that compound **5g** induced apoptosis in Hela through ROS-mediated mitochondrial dysfunction signaling pathways.

1. Introduction

Cancer continues to be a major threat to human health and is regarded as one of the most common causes of death worldwide. Although significant achievements have been made in anticancer agents, identifying effective, safe, and novel chemical entities is still a big challenge. Inducing cell apoptosis has been an effective method for tumor treatment. It is well recognized that the apoptotic pathways mainly involve two routes: the mitochondrial apoptosis pathway and the death receptor pathway. As signaling molecules, reactive oxygen species (ROS) are effective in mediating multiple biological events, including cellular survival and death [1,2]. Moreover, mitochondria are, to a great extent, considered the major source of ROS production [3]. High levels of ROS can mediate cell apoptosis, and even necrosis, through mitochondrial dysfunction, loss of Mitochondrial membrane potential (Δψm), the release of cytochrome *C* (Cyt *C*), cleavage of executioner caspases-3/9, and levels of the Bcl-2 family proteins [4–11]. Together, those events ultimately result in cell apoptosis.

Essential oils and their derivatives, well known for medicinal purposes [12], play an important role in drug discovery. For example, turpentine, obtained from resin, has been used as permeation enhancer [13] and therapeutic agents [14–16] in drugs. β-Pinene, which is isolated from the raw material of turpentine, is a consequential natural monoterpene resource that is widely used for producing natural perfume [17]. Additionally, β-pinene is an important raw material for industrial synthesis. β-Pinene derivatives have wide spread biological activities, including anticancer, antibacterial, anticoagulation, and antimalarial activities [18–21]. Over the last few decades, the application of β-pinene mainly concentrated on spices, and studies on β-pinene pharmaceuticals were limited. Therefore, studying the pharmacological effects of β-pinene and its derivatives is a field that is wide open and may have great potential.

The α, β-Unsaturated carbonyl structures have been recognized as one of the privileged structures in drug discovery and were widely distributed in biologically active compounds that have successfully been applied in cancer therapeutics [22,23] due to its low genotoxic

* Corresponding authors at: College of Chemical Engineering, Nanjing Forestry University, Nanjing 210037, PR China.
E-mail address: wangshifa65@163.com (S. Wang).

https://doi.org/10.1016/j.bioorg.2018.12.010
Received 4 September 2018; Received in revised form 27 November 2018; Accepted 8 December 2018
Available online 10 December 2018
0045-2068/

effects and limited reactivity toward cell hydroxyl or amino groups of functional ketone groups [24,25]. In addition, the functional C═N group, as the necessary component of Schiff bases, is present in several bioactive molecules, and is recognized as a key building block for the synthesis of small-molecules with potential pharmaceutical activities [26–28]. Therefore, building functional C═N groups based on the *α*, *β*-unsaturated carbonyl structure has high potential.

Moreover, heterocyclic groups, such as thiazole, are considered a widely-distributed framework that is present in many pharmaceuticals and natural compounds. Thiazole and its derivatives have been proven pharmacologically important heterocyclic nucleus in anti-HIV [29], antibacterial [30], antimalarial [31], and anti-inflammatory [32] territories. In particular, the use of thiazole hydrazone scaffolds as an active framework in the design of anticancer agents has been the focus of numerous studies [33–35]. In most cases, the antitumor mechanism of action of thiazole derivatives was limited to a mitochondria-dependent pathway [36,37]. Therefore, a series of substituted thiazoles was synthesized and connected with the pinene moiety via the C═N group.

Our studies have long been fully committed to the synthesis of novel turpentine derivatives and their application in chemistry and biology, such as anticancer [38,39], antimicrobial [40], insecticidal activities [41], and fluorescent dyes [42,43]. Among them, many compounds exhibited potent antitumor activities, especially *β*-pinene based thiosemicarbazone derivatives [44], which showed strong inhibitory activity on the proliferation of MDA-MB-231, SMMC-7721, and Hela cells. In addition, it has been rarely reported that thiazole derivatives were synthesized from *α,β*-unsaturated ketone. Encouraged by the above results and in continuation of our program, which is aimed at the development of potential anticancer agents, in this study we designed and synthesized *β*-pinene-based thiazole derivatives and studied their antitumor activities against human cancer cell lines *in vitro*. In addition, we also preliminarily probed the underlying antitumor mechanisms of the derivatives.

2. Results and discussion

2.1. Synthesis and characterization

The protocol for the synthesis of thiazole derivatives **5a–5x** from *β*-pinene **1** involves four steps, including oxidation, aldol condensation, addition condensation and Hantzsch cyclization reactions (see Scheme 1). Compound **1** was treated with potassium permanganate in acetone at 0 °C to form nopinone **2**. Intermediates **3** were generated by aldol condensation of nopinone **2** with substituted benzaldehydes in excellent yields using sodium ethoxide as the catalyst. Subsequently, compounds **4** were prepared by condensation of intermediates **3** and thiosemicarbazide using hydrochloric acid as the catalyst. The novel thiazole derivatives **5a–5x** were prepared by cyclization of compounds **4** with phenacyl bromide. The structures of target compounds were characterized by ^{1}H NMR, ^{13}C NMR and HRMS. As exemplified with the ^{1}H NMR analysis of 4-(2-(2-(3-benzylidene-6,6-dimethylbicyclo [3.1.1] heptan-2-ylidene) hydrazinyl) thiazol-4-yl) phenol (**5f**), singlet and doublets peaks, corresponding to aromatic protons, were observed at *δ* 7.16–8.26. For the thiazole ring, a singlet at *δ* 7.57 was found. NH proton appeared as singlet at *δ* 12.59. ^{13}C NMR spectrum of **5f** showed peaks of the aromatic carbons were found at *δ* 115.73–146.74 ppm. The presence of peaks at *δ* 123.74 and 169.49 ppm, confirm the thiazole cyclisation. Besides, representative ^{1}H NMR and ^{13}C NMR spectrums of some compounds are presented in Supplementary Material.

2.2. Anti-proliferative activity of thiazole derivatives (5a–5x) by MTT assay

The designed 24 compounds were evaluated for cytotoxicity against three cancer cell lines (colon cancer CT-26 cells, human cervical carcinoma Hela cells and human hepatocarcinoma SMMC-7721 cells) using the MTT assay with etoposide as a positive control. As illustrated in Table 1, most designed compounds exhibited cytotoxic activities against the selected cells. Among them, six compounds (**5c**, **5g**, **5k**, **5o**, and **5w**) showed strong inhibitory effects against the three cancer cell lines selected. In addition, it was observed that the activities of compounds **5c** and **5w** were slightly weaker towards SMMC-7721 cells when compared to other hydroxy-substituted compounds (**5g**, **5k**, and **5o**). Moreover, we found that compound **5g** was the most effective in cervical cancer (Hela) cells. Additionally, several other compounds, including compounds **5d**, **5h**, and **5x** showed moderate anti-cancer activities, whereas eight compounds (**5f**, **5j**, **5m**, **5n**, **5q**, **5r**, **5t**, and **5v**) did not show any promising anti-cancer activity *in vitro*.

The activity results of compounds **5c**, **5g**, **5k**, **5o** and **5w** showed that compounds bearing a strong electron-donating group (R_2 = OH) in the *para*-position (Table 1) were more active against a wide range of tumor cell lines (CT-26, SMMC-7721, and Hela cells) when compared with other substituent groups. Especially, compound **5g** in which the electron-acceptor group (R_1 = NO_2) was present, showed a lower IC_{50} value ranging from 3.48 μM to 8.84 μM. Moreover, the electron-withdrawing group (R_2 = F) greatly reduced the activity of the corresponding derivatives and even lost their antitumor activities as reflected by compound **5b** with an IC_{50} value ranging from 30.44 μM to

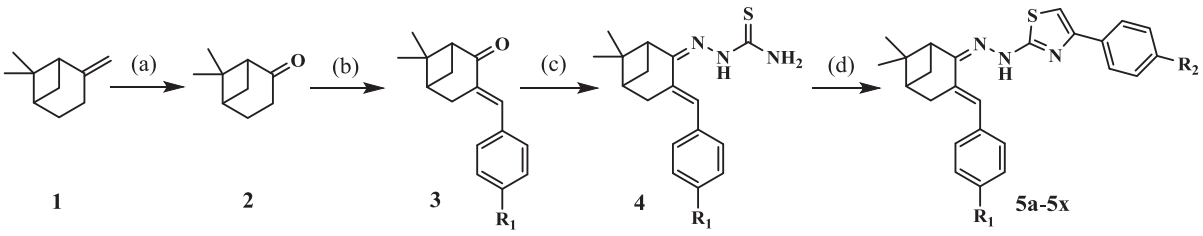

5a: R_1= H, R_2= H
5b: R_1= H, R_2= F
5c: R_1= H, R_2= OH
5d: R_1= H, R_2= OCH_3
5e: R_1= NO_2, R_2= H
5f: R_1= NO_2, R_2= F
5g: R_1= NO_2, R_2= OH
5h: R_1= NO_2, R_2= OCH_3
5i: R_1= F, R_2= H
5j: R_1= F, R_2= F
5k: R_1= F, R_2= OH
5l: R_1= F, R_2= OCH_3
5m: R_1= OCH_3, R_2= H
5n: R_1= OCH_3, R_2= F
5o: R_1= OCH_3, R_2= OH
5p: R_1= OCH_3, R_2= OCH_3
5q: R_1= CH_3, R_2= H
5r: R_1= CH_3, R_2= F
5s: R_1= CH_3, R_2= OH
5t: R_1= CH_3, R_2= OCH_3
5u: R_1= Cl, R_2= H
5v: R_1= Cl, R_2= F
5w: R_1= Cl, R_2= OH
5x: R_1= Cl, R_2= OCH_3

Scheme 1. Synthesis of *β*-pinene-based thiazole derivatives **5a–5x**. Reagents and experimental conditions were as follows: (a) $KMnO_4$, H_2SO_4, acetone, ice bath to room temperature, 6 h. (b) substituted benzaldehyde, C_2H_5ONa, ethanol, reflux, 8 h. (c) HCl, ethanol, reflux, 4–6 h. (d) phenacyl bromide, reflux.

Table 1
Antiproliferative activities of compounds **5a–5x**.

Compounds	R_1	R_2	IC_{50}(μM)		
			Hela	CT-26	SMMC-7721
5a	H	H	21.19 ± 0.23	21.66 ± 0.12	66.94 ± 0.0.69
5b	H	F	30.44 ± 0.05	45.51 ± 0.09	52.52 ± 0.05
5c	H	OH	5.99 ± 0.14	7.15 ± 0.11	12.98 ± 0.52
5d	H	OCH_3	13.40 ± 0.16	16.40 ± 0.1.7	31.15 ± 0.12
5e	NO_2	H	33.33 ± 0.23	25.04 ± 0.04	50.47 ± 0.13
5f	NO_2	F	> 80	> 80	> 80
5g	NO_2	OH	3.48 ± 0.14	8.84 ± 0.16	6.69 ± 0.15
5h	NO_2	OCH_3	19.91 ± 0.19	44.55 ± 0.76	41.62 ± 0.09
5i	F	H	37.79 ± 0.05	33.75 ± 0.10	> 80
5j	F	F	> 80	> 80	67.41 ± 0.12
5k	F	OH	3.57 ± 0.11	9.01 ± 0.21	19.42 ± 0.12
5l	F	OCH_3	42.97 ± 0.47	39.95 ± 0.06	30.26 ± 0.06
5m	OCH_3	H	> 80	> 80	> 80
5n	OCH_3	F	> 80	> 80	> 80
5o	OCH_3	OH	8.813 ± 0.19	10.71 ± 0.11	9.76 ± 0.07
5p	OCH_3	OCH_3	41.34 ± 0.03	38.45 ± 0.07	30.3 ± 0.07
5q	CH_3	H	> 80	> 80	> 80
5r	CH_3	F	> 80	> 80	> 80
5s	CH_3	OH	8.224 ± 0.05	5.89 ± 0.07	7.46 ± 0.11
5t	CH_3	OCH_3	> 80	> 80	> 80
5u	Cl	H	33.35 ± 0.20	48.82 ± 0.10	42.03 ± 0.16
5v	Cl	F	> 80	> 80	> 80
5w	Cl	OH	6.46 ± 0.16	8.95 ± 0.17	14.69 ± 0.07
5x	Cl	OCH_3	17.55 ± 0.03	30.61 ± 0.20	39.09 ± 0.03
Etoposide	–	–	7.89 ± 1.37	2.22 ± 1.26	40.44 ± 0.29

52.52 μM. When the electron-donating group (CH_3, OCH_3) was introduced into the R_1 position, most compounds (**5m**, **5n**, **5q**, **5r**, and **5t**) were inactive. Interestingly, when a non-substituted group was present at the R_1 position, compounds (**5a–5d**) obtained prominent antitumor activities.

2.3. Apoptosis analysis by flow cytometry assay

Cell apoptosis analysis was carried out to evaluate whether the growth inhibitory effects of these compounds on tumor cells were caused by cell apoptosis. Accordingly, compound **5g** was selected for Annexin V/PI apoptosis assay due to its high anticancer activity in the MTT assay. In brief, Hela cells were treated with different doses of compound **5g** for 72 h and evaluated for apoptosis by flow cytometry using an Annexin V-APC/PI assay. Fig. 1 shows a significant increase in apoptosis events at 2.5 μM of compound **5g** when compared to the control. In addition, the cell apoptosis rate increased when the radiation dose was increased. Combined, these results suggested that compound **5g** induced apoptosis in Hela cells in a dose-dependent manner.

2.4. Investigation of cell cycle distribution

To further investigate the antitumor mechanism of action, the effect of compound **5g** on the cell cycle was evaluated. Hela cells were harvested after treatment with compound **5g** and analyzed by flow cytometry using PI-stained cell populations. The consequent cell cycle distributions are presented in Fig. 2. Hela cells treated with a low dose (2.5 μM) of compound **5g** showed an increase in the G0/G1 phase cell population at the expense of reducing the S phase population when compared to the control. This accumulation in G0/G1 phase was maintained by increasing the **5g** concentration to 5 μM and 10 μM, respectively. Together, these results indicated that compound **5g** caused significant G0/G1 phase arrest.

2.5. Intracellular ROS level in dose-dependent manner

ROS act as part of a secondary messenger in cellular signaling and are closely related to cell survival and cell death. High ROS levels can cause mitochondrial dysfunction, resulting in apoptosis of cancer cells

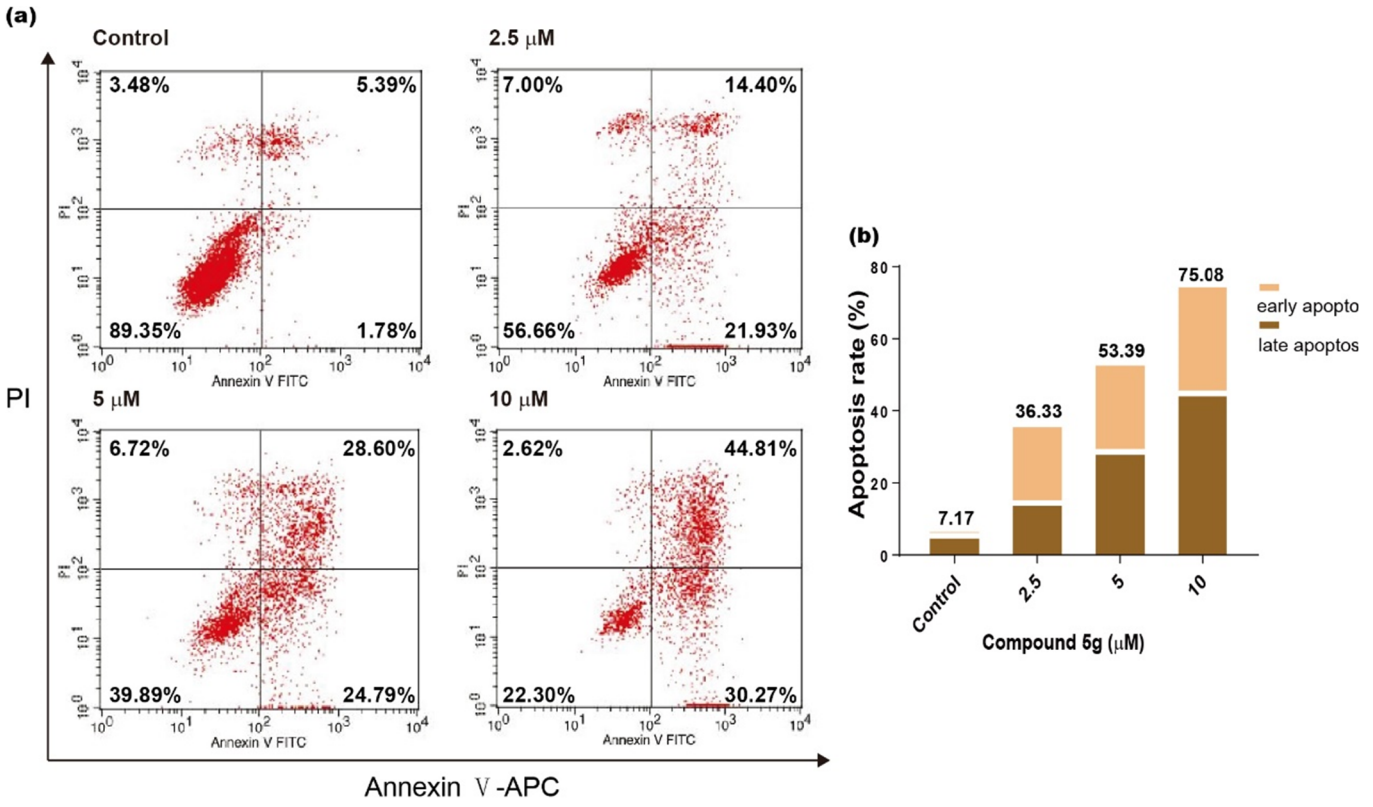

Fig. 1. Flow cytometric analysis of Hela cells treated with compounds **5g**. (a) exposure to 2.5, 5 and 10 μM of compound **5g** for 72 h and detection and analysis of cell cycle by flow cytometry. (b) the apoptosis rate in undergone treated by compound **5g**.

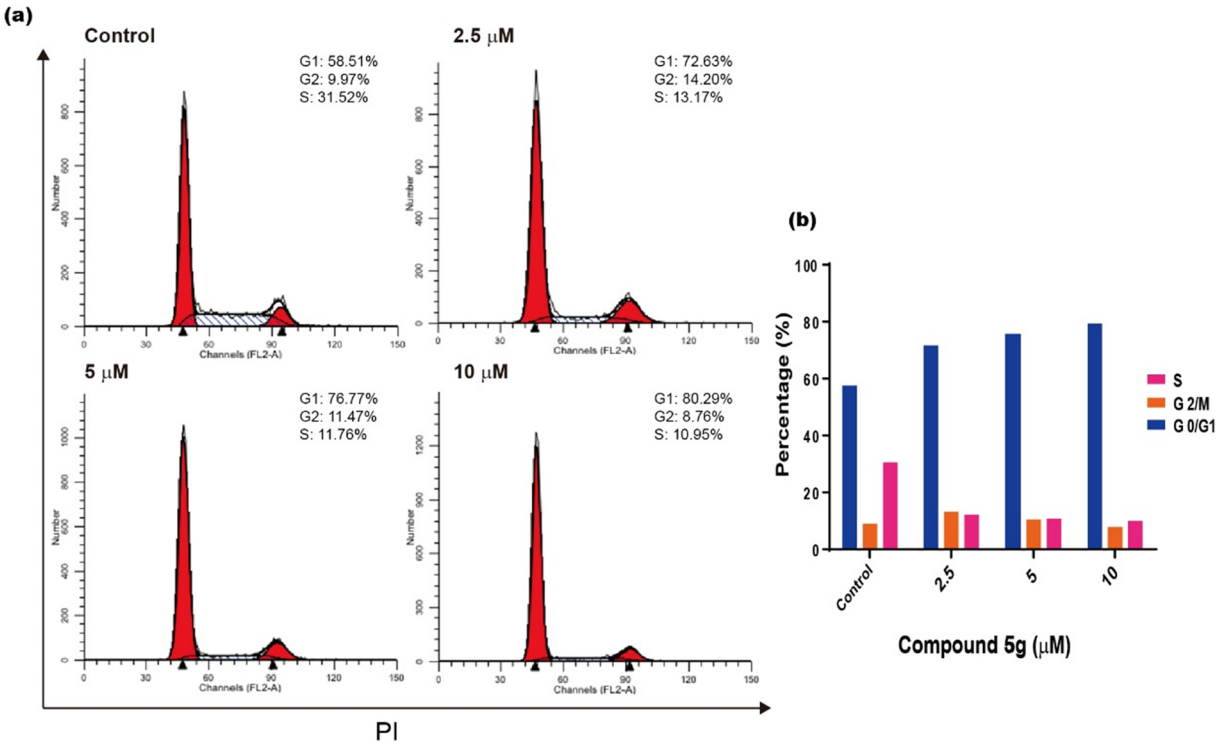

Fig. 2. Cell cycle distribution of Hela cells (a) exposure to 2.5, 5 and 10 μM of compound **5g** for 24 h and detection and analysis of cell cycle by flow cytometry. (b) the cell cycle change in undergone treated by compound **5g**.

[45]. To evaluate whether *β*-pinene-based thiazole derivatives induced ROS accumulation in Hela cells, flow cytometric analysis and microscopic fluorescence imaging were conducted. In brief, Hela cells were incubated with different concentrations of compound **5g** (2.5, 5, and 10 μM). As shown in Fig. 3, imaging analysis revealed that compound **5g** strongly generated ROS in a dose-dependent manner. It was found that treatment with **5g** resulted in an increase in DCF fluorescence intensity when compared to untreated control cells. Therefore, these results suggested that compound **5g** triggered the production and accumulation of intracellular ROS in Hela cells in a dose-dependent manner.

2.6. Measurement of mitochondrial membrane potential

Mitochondria, as the energy center of the cell, are closely connected with cell apoptotic events. Mitochondrial dysfunction is one of the most profound features of apoptosis and involves the process, such as mitochondrial permeability transition or the reduction of mitochondrial membrane potential (MMP) [46]. In this study, mitochondrial dysfunction was determined based on the MMP index that was measured by flow cytometry using JC-1 dye as a fluorescent probe. As shown in Fig. 4, after exposure to 2.5, 5, or 10 μM of compound **5g** for 72 h, **5g**-treated Hela cells exhibited notably increased green fluorescence and the proportion of green fluorescence increased from 28.62% to 65.70%. These results indicated that compound **5g** could reduce the mitochondria membrane potential of the cells, resulting in a dose-dependent loss in membrane potential. As a consequence, **5g**-induced apoptosis involved the mitochondrial pathway.

2.7. Western blot analysis

As shown previously, compound **5g** induced a loss of $\Delta\Psi m$ in Hela cells. These results suggested that the mitochondrial apoptosis pathway participated in **5g**-induced Hela cell apoptosis. In the course of mediating apoptosis of cancer cells through the mitochondrial pathway, mitochondria release Cyt *C* into the cytosol, which is followed by induction of apoptosis factors and activation of caspases [47]. The expression of apoptosis protein in Hela cells after treatment with compound **5g** for 72 h was detected by Western blot analysis. As shown in Fig. 5, the immunoblot results confirmed that treatment with compound **5g** decreased Bcl-2 expression, and increased Bax in a concentration-dependent manner. As illustrated in Fig. 5(b), the proportion of Bax/Bcl-2 increased, indicating that compound **5g** induced apoptosis by elevating the ratio of Bax/Bcl-2. Moreover, caspase-3 and caspase-9 are the most important signaling proteins associated with the mitochondria-mediated apoptosis pathway. The expression of cleaved caspase-3 is a biochemical marker of apoptosis[19]. Fig. 5(a) and (c) show that after treatment with compound **5g**, the expression of cleaved caspase-3, caspase-9, and Cyt *C* was increased when compared to that in control cells. In summary, our results demonstrated that compound **5g** induced apoptosis by regulating Bcl-2, Bax, caspase-3, caspase-9, and Cyt *C* expression.

3. Conclusion

In this study, 24 thiazole analogues were designed, synthesized, and evaluated for antiproliferative activities. MTT analysis indicated that the antitumor properties of thiazole containing a hydroxyl group on the phenyl group were increased, and that when thiazole contained a fluorine-group, it was decreased. Among the compounds, compound **5g** showed the highest activity (3.48 μM) on Hela cells. These findings indicated that thiazole with a hydroxyl group on the phenyl group was favorable for increasing of anti-cancer activity by structural optimization. Mechanistic studies showed that compound **5g** induced the formation of ROS, decreased the mitochondrial membrane potential and released Cyt *C* into the cytoplasm. Moreover, compound **5g** arrested the cell cycle in the G0/G1 phase and induced cancer cells to be in early apoptosis, thereby altering the expression of Bax/Bcl-2 proteins. Together, these findings indicated that compound **5g** induced apoptosis via the mitochondria-mediated apoptosis pathway.

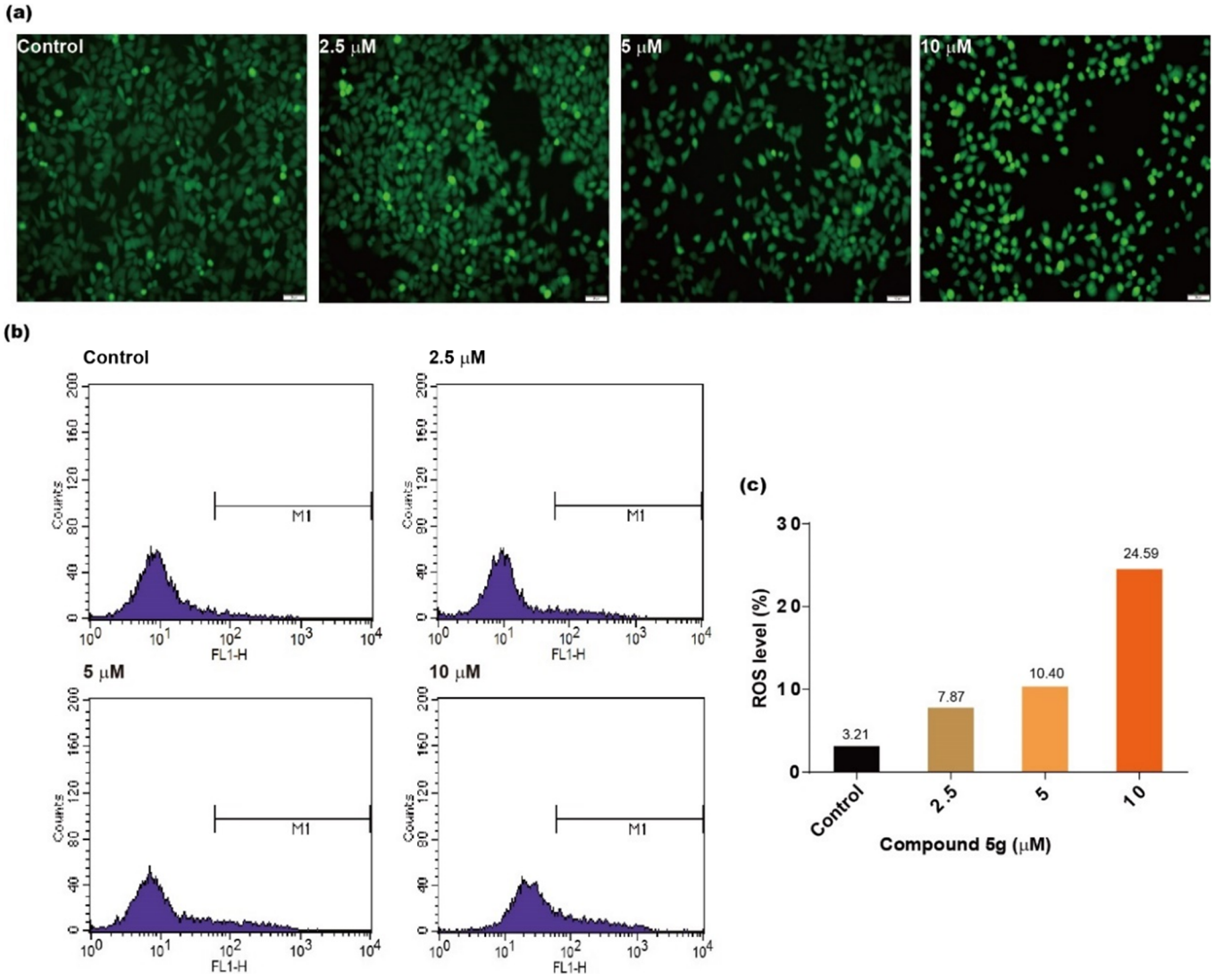

Fig. 3. (a) HeLa cells were incubated with 0, 2.5, 5 and 10 μM of compound **5g** for 72 h and intracellular DCF fluorescence were observed by fluorescent microscope. (b) intracellular ROS level were determined by flow cytometry. (c) ROS levels after exposing HeLa cells for 72 h and distinctly higher ROS levels compared to untreated control cells.

4. Experimental

4.1. Chemistry

The reagents (chemicals), all being of A.R. grade, were purchased from Energy Chemical Reagent Company, Aladdin Reagent Company or Shanghai Chemical Reagent Company (Shanghai, China). Reactions were monitored by thin layer chromatography (TLC), which was carried out on silica gel IB-F flexible sheets from Mallinckrodt Baker Inc., Germany, and visualized in UV light (254 nm). Silica gel (200–300 mesh) for column chromatography was purchased from Qingdao Marine Chemical Factory (Qingdao, China). Nuclear magnetic resonance (^{1}H NMR and ^{13}C NMR) spectra were accomplished in $CDCl_3$ or C_5D_5N on Bruker AV-400 and AV-500 NMR spectrometers using TMS as internal standard. The HR-MS spectra were recorded on Agilent 6540 high-resolution mass spectrometer.

4.1.1. Synthesis of nopinone (2)

Nopinone (**2**) was synthesized according to a previous published method [48]. In brief, 30 mL H_2SO_4 (2 mol/L) was added to 250 mL acetone solution containing 0.41 mol β-pinene (**1**) in an ice bath. Then 1.10 mol $KMnO_4$ powder was slowly added to the above solution, and the reaction was maintained at room temperature for 6 h. After completion of reaction, solid particles were filtered from the solution, washed with acetone, and the acetone solution was collected. After removing the solvent by reduced pressure distillation, the residue was diluted with 40 mL cyclohexane, washed with distilled water, saturated to neutrality with brine, and dried with anhydrous sodium sulfate. Nopinone was obtained as a yellowish limpid liquid through evaporating cyclohexane (yield 80%).

4.1.2. Synthesis of compounds *3*

A total of 13.7 mmol sodium ethoxide and corresponding substituted benzaldehyde (1.1 eq, 15.1 mol) was added to a solution of nopinone **2** (13.7 mmol) in ethanol, and the resulting mixture was refluxed with stirring for 8 h. After cooling, the solvent was removed under reduced pressure. The crude products were separated by silica gel (200–300 mesh) column chromatography and eluted with ethyl acetate and petroleum ether (v: v = 3:1; yield 85%).

4.1.3. Synthesis of compounds *4*

Compounds **3** (2 mmol) reacted with thiosemicarbazide (2 mmol) in the presence of 0.5 mL HCl in absolute ethyl alcohol (20 mL) at reflux temperature. At completion of the reaction, the obtained concentrated

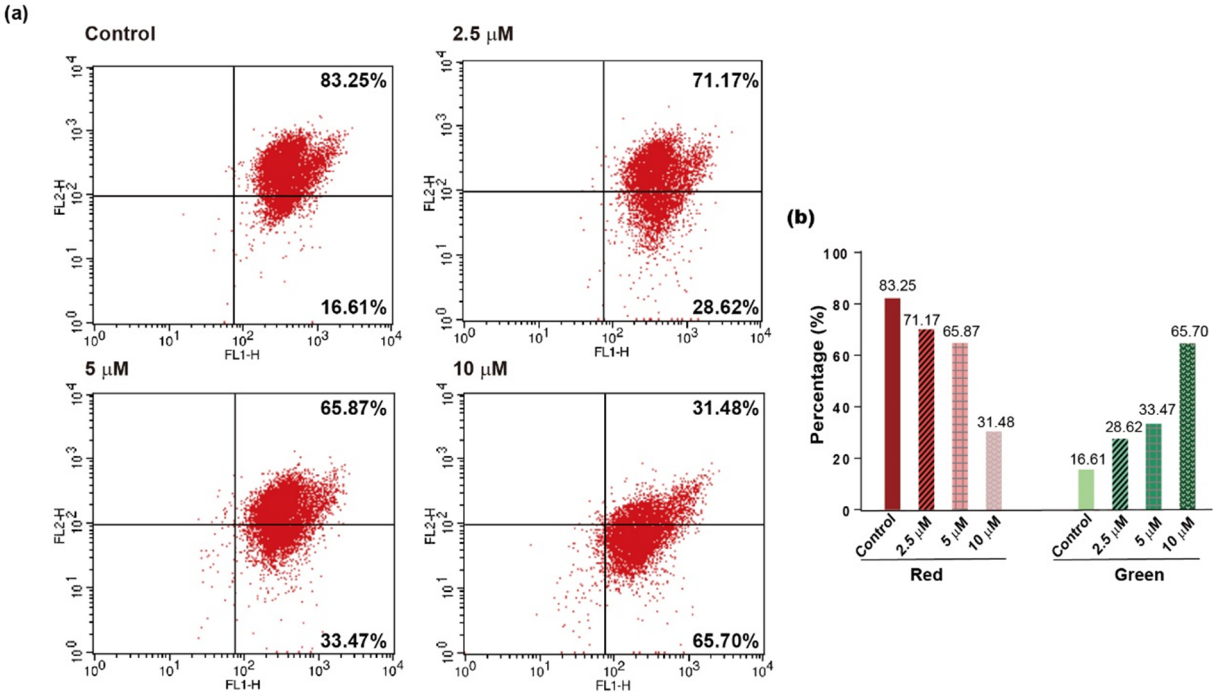

Fig. 4. HeLa cells after incubation with compound **5g** in 2.5, 5 and 10 μM for 72 h. (a) the MMP was measured by flow cytometry. (b) the percentages of loss of mitochondrial membrane potential in Hela cells induced by different concentrations of compound **5g**.

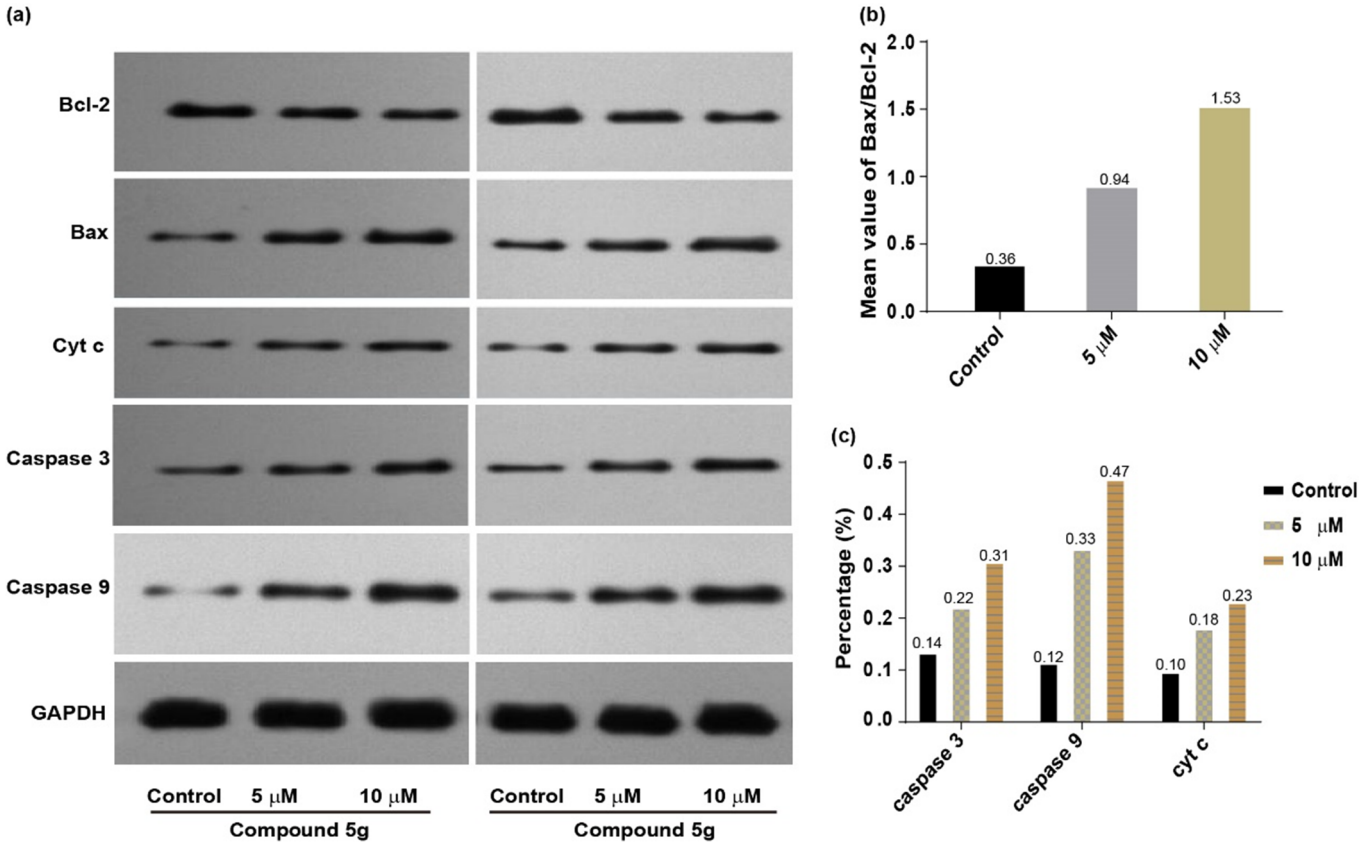

Fig. 5. The expression of Cyt *C*, caspases and Bcl-2 family proteins in Hela cells induced by 5 and 10 μM of compound **5g** for 72 h, GAPDH was used to internal control. (a) the expression of caspases and Bcl-2 family proteins detected by western blot; (b) the rate changes of Bax/Bcl-2 in treated Hela cells; (c) compound **5g** induced the rise of Cyt *C*, caspases and Bcl-2 family proteins levels in Hela cells.

reaction solution was purified by a silica column using *n*-hexane/EtOAc (8:1) to generate targeted compounds **4** (yield 80%).

*4.1.4. Synthesis of target compounds **5***

An equimolar mixture of bromoacetophenone and compounds **4** (3.3 mmol) were dissolved in 20 mL ethanol and stirred for 2 h at room temperature. During the reaction process, the reaction mixture turned into powder and remained suspended in solution. The powder was filtered and washed with 5 mL petroleum ether to generate compounds **5a–5x**.

*4.1.4.1. 2-(2-(3-benzylidene-6,6-dimethylbicyclo[3.1.1]heptan-2-ylidene) hydrazinyl)-4-phenylthiazole (**5a**)*. Yield 78.4%; m.p. 176.5–179.6 °C. ^{1}H NMR (400 MHz, $CDCl_3$) δ: 7.71 (m, 2H), 7.50 (s, 1H), 7.40 (d, J = 8.0 Hz, 2H), 7.20 (d, J = 8.0 Hz, 2H), 7.15 (t, J = 8.6 Hz, 2H), 6.67 (s, 1H), 3.55 (t, J = 5.4 Hz, 1H), 2.92 (s, 2H), 2.61 (m, 1H), 2.37 (s, 3H), 2.22 (m, 1H), 1.49 (s, 3H), 1.33 (d, J = 10.4 Hz, 1H), 0.93 (s, 3H); ^{13}C NMR (100 MHz, $CDCl_3$) δ: 169.38, 165.86, 140.59, 136.36, 130.99, 130.70, 130.40, 130.14, 129.64, 128.52, 128.17, 125.65, 100.82, 44.52, 42.34, 39.41, 31.75, 27.87, 26.10, 21.66. HR-MS (ESI^+): *m/z* calculated for $C_{25}H_{25}N_3S$ $[M+H]^+$ 400.1847, found 400.1853.

*4.1.4.2. 2-(2-(3-benzylidene-6,6-dimethylbicyclo[3.1.1]heptan-2-ylidene) hydrazinyl) −4-(4-fluorophenyl)thiazole (**5b**)*. Yield 85.2%; m.p. 205.3–206.3 °C. ^{1}H NMR (400 MHz, $CDCl_3$) δ: 12.56 (s, 1H), 7.74 (dd, J = 8.7, 5.0 Hz, 2H), 7.50 (m, 3H), 7.43 (t, J = 7.6 Hz, 2H), 7.31 (m, 1H), 7.19 (t, J = 8.5 Hz, 2H), 6.70 (s, 1H), 3.60 (t, J = 5.4 Hz, 1H), 2.97 (d, J = 2.8 Hz, 2H), 2.65 (m, 1H), 2.26 (m, 1H), 1.37 (d, J = 10.4 Hz, 1H), 0.97 (s, 3H); ^{13}C NMR (100 MHz, $CDCl_3$) δ: 169.31, 165.91, 139.57, 136.27, 131.00, 130.58, 130.07, 128.46, 128.13, 127.76, 127.67, 123.76, 116.92, 116.70, 100.44, 44.43, 42.30, 39.34, 31.66, 27.80, 26.04, 21.59. HR-MS (ESI^+): *m/z* calculated for $C_{25}H_{24}FN_3S$ $[M+H]^+$ 418.1753, found 418.1761.

*4.1.4.3. 4-(2-(2-(3-benzylidene-6,6-dimethylbicyclo[3.1.1]heptan-2-ylidene)hydrazinyl)thiazol-4-yl)phenol (**5c**)*. Yield 81.3%; m.p. 132.6–133.2 °C.^{1}H NMR (400 MHz, C_5D_5N) δ: 8.08 (d, J = 8.6 Hz, 2H), 7.61 (d, J = 7.4 Hz, 2H), 7.90 (s, 1H), 7.30 (t, J = 8.9 Hz, 3H), 7.45 (t, J = 7.7 Hz, 2H), 7.10 (s, 1H), 3.79 (t, J = 5.6 Hz, 1H), 2.92 (m, 1H), 2.83 (m, 1H), 2.46 (m, 1H), 2.04 (m, 1H), 1.24 (s, 3H), 1.22 (s, 1H), 0.84 (s, 3H); ^{13}C NMR (100 MHz, C_5D_5N) δ: 170.73, 158.57, 154.83, 151.73, 137.57, 132.47, 130.01, 128.64, 127.69, 127.33, 127.25, 127.14, 116.22, 100.70, 42.66, 40.98, 39.57, 32.02, 28.18, 25.72, 21.29. HR-MS (ESI^+): *m/z* calculated for $C_{25}H_{25}N_3OS$ $[M+H]^+$ 416.1797, found 416.1776.

*4.1.4.4. 2-(2-(3-benzylidene-6,6-dimethylbicyclo[3.1.1]heptan-2-ylidene) hydrazinyl)-4-(4-methoxyphenyl)thiazole (**5d**)*. Yield 81.0%; m.p. 132.6–133.2 °C.^{1}H NMR (400 MHz, $CDCl_3$) δ: 12.55 (s, 1H), 7.66 (m, 2H), 7.53 (m, 3H), 7.41 (dd, J = 8.4, 6.8 Hz, 2H), 7.34 (m, 1H), 6.99 (m, 2H), 6.59 (s, 1H), 3.84 (s, 3H), 3.61 (t, J = 5.4 Hz, 1H), 3.01 (m, 2H), 2.55 (m, 1H), 2.24 (m, 1H), 1.52 (s, 3H), 1.36 (d, J = 10.4 Hz, 1H), 0.96 (s, 3H); ^{13}C NMR (100 MHz, $CDCl_3$) δ: 169.28, 165.54, 161.18, 140.48, 136.41, 130.87, 130.74, 130.14, 128.52, 128.14, 127.20, 120.13, 115.01, 98.64, 55.53, 44.43, 42.31, 39.42, 31.76, 27.88, 26.10, 21.66. HR-MS (ESI^+): *m/z* calculated for $C_{26}H_{27}N_3OS$ $[M+H]^+$ 430.1953, found 430.1957.

*4.1.4.5. 2-(2-(6,6-dimethyl-3-(4-nitrobenzylidene)bicyclo[3.1.1]heptan-2-ylidene)hydrazinyl)-4-phenylthiazole (**5e**)*. Yield 87.2%; m.p. 206.4–207.1 °C. ^{1}H NMR (400 MHz, $CDCl_3$) δ: 12.76 (s, 1H), 8.26 (d, J = 8.8 Hz, 2H), 7.72 (d, J = 6.8 Hz, 2H), 7.66 (d, J = 8.8 Hz, 2H), 7.47 (m, 3H), 7.58 (s, 1H), 6.80 (s, 1H), 3.67 (t, J = 5.3 Hz, 1H), 3.00 (m, 1H), 2.94 (m, 1H), 2.69 (m, 1H), 2.29 (m, 1H), 1.53 (s, 3H), 1.36 (d, J = 10.6 Hz, 1H), 0.96 (s, 3H); ^{13}C NMR (100 MHz, $CDCl_3$) δ: 169.60, 164.74, 142.77, 140.85, 135.02, 130.59, 130.56, 129.70, 128.41, 125.68, 123.77, 100.98, 44.59, 42.41, 39.25, 31.93, 27.92, 26.00, 21.68. HR-MS (ESI^+): *m/z* calculated for $C_{25}H_{24}N4O_2S$ $[M+H]^+$ 445.1698, found 445.1696.

*4.1.4.6. 2-(2-(6,6-dimethyl-3-(4-nitrobenzylidene)bicyclo[3.1.1]heptan-2-ylidene)hydrazinyl)-4-(4-fluorophenyl)thiazole (**5f**)*. Yield 83.7%; m.p. 207.5–208.5 °C. ^{1}H NMR (400 MHz, $CDCl_3$) δ: 12.59 (s, 1H), 8.25 (d, J = 8.7 Hz, 2H), 7.73 (dd, J = 8.8, 5.0 Hz, 2H), 7.65 (d, J = 8.8 Hz, 2H), 7.57 (s, 1H), 7.18 (t, J = 8.5 Hz, 2H), 6.77 (s, 1H), 3.63 (t, J = 5.4 Hz, 1H), 3.02 (m, 2H), 2.68 (m, 1H), 2.28 (m, 1H), 1.52 (s, 3H), 1.36 (d, J = 10.6 Hz, 1H), 0.96 (s, 3H); ^{13}C NMR (100 MHz, $CDCl_3$) δ: 169.49, 164.72, 146.74, 142.64, 139.71, 134.85, 130.51, 128.39, 127.79, 127.70, 123.67, 116.95, 116.73, 100.81, 44.45, 42.34, 39.16, 31.82, 27.82, 25.92, 21.59. HR-MS (ESI^+): *m/z* calculated for $C_{25}H_{24}N_4O_2FS$ $[M+H]^+$ 445.1698, found 445.1696.

*4.1.4.7. 4-(2-(2-(6,6-dimethyl-3-(4-nitrobenzylidene)bicyclo[3.1.1] heptan-2-ylidene)hydrazinyl)thiazol-4-yl)phenol (**5g**)*. Yield 70.6%; m.p. 132.6–133.2 °C. ^{1}H NMR (400 MHz, C_5D_5N) δ: 8.29 (d, J = 8.9 Hz, 2H), 8.08 (d, J = 8.4 Hz, 2H), 7.84 (s, 1H), 7.67 (d, J = 8.6 Hz, 2H), 7.28 (d, J = 8.6 Hz, 2H), 7.13 (s, 1H), 3.81 (t, J = 5.6 Hz, 1H), 2.94 (m, 1H), 2.84 (m, 1H), 2.51 (m, 1H), 2.08 (tt, J = 3.0, 6.0 Hz, 1H), 1.26 (s, 3H), 1.23 (s, 1H), 0.85 (s, 3H); ^{13}C NMR (100 MHz, C_5D_5N) δ: 171.92, 160.14, 155.25, 153.20, 147.59, 145.48, 138.57, 131.85, 129.21, 128.61, 126.26, 117.73, 102.39, 44.12, 42.43, 40.94, 33.72, 29.81, 27.11, 22.77. HR-MS (ESI^+): *m/z* calculated for $C_{25}H_{24}N_4O_3S$ $[M+H]^+$ 461.1647, found 461.1642.

*4.1.4.8. 2-(2-(6,6-dimethyl-3-(4-nitrobenzylidene)bicyclo[3.1.1]heptan-2-ylidene)hydrazinyl)-4-(4-methoxyphenyl)thiazole (**5h**)*. Yield 77.1%; m.p. 143.8–146.1 °C. ^{1}H NMR (400 MHz, $CDCl_3$) δ: 12.68 (s, 1H), 8.25 (dd, J = 11.0, 8.7 Hz, 4H), 7.62 (d, J = 8.7 Hz, 2H), 7.51 (s, 1H), 7.00 (d, J = 8.8 Hz, 2H), 3.86 (s, 3H), 3.67 (m, 1H), 2.99 (m, 2H), 2.70 (m, 1H), 2.28 (s, 1H), 1.54 (s, 3H), 1.37 (d, J = 9.2 Hz, 1H), 0.97 (s, 3H); ^{13}C NMR (100 MHz, $CDCl_3$) δ: 169.38, 164.34, 161.22, 156.01, 146.72, 142.92, 135.55, 130.32, 128.21, 127.16, 126.72, 123.67, 115.00, 98.59, 55.48, 42.31, 41.73, 39.23, 31.92, 27.87, 26.00, 21.51. HR-MS (ESI^+): *m/z* calculated for $C_{26}H_{26}N_4O_3S$ $[M+H]^+$ 474.1726, found 474.1696.

*4.1.4.9. 2-(2-(3-(4-fluorobenzylidene)-6,6-dimethylbicyclo[3.1.1]heptan-2-ylidene)hydrazinyl)-4-phenylthiazole (**5i**)*. Yield 80.4%; m.p. 194.7–196.2 °C. ^{1}H NMR (400 MHz, $CDCl_3$) δ: 12.59 (s, 1H), 7.70 (d, J = 7.8 Hz, 2H), 7.45 (m, 6H), 7.36 (d, J = 8.5 Hz, 2H), 6.79 (s, 1H), 3.62 (t, J = 5.4 Hz, 1H), 2.90 (m, 2H), 2.63 (dt, J = 10.5, 5.5 Hz, 1H), 2.24 (m, 1H), 1.50 (s, 3H), 1.33 (d, J = 10.4 Hz, 1H), 0.94 (s, 3H); ^{13}C NMR (100 MHz, $CDCl_3$) δ: 169.31, 165.31, 140.52, 134.73, 133.86, 131.25, 130.31, 129.55, 129.50, 128.65, 127.33, 125.55, 100.94, 44.41, 42.25, 39.26, 31.67, 27.81, 25.99, 21.57. HR-MS (ESI^+): *m/z* calculated for $C_{25}H_{24}FN_3S$ $[M+H]^+$ 418.1753, found 418.1753.

*4.1.4.10. 2-(2-(3-(4-fluorobenzylidene)-6,6-dimethylbicyclo[3.1.1] heptan-2-ylidene)hydrazinyl)-4-(4-fluorophenyl)thiazole (**5j**)*. Yield 81.9%; m.p. 196.4–196.9 °C. ^{1}H NMR (400 MHz, $CDCl_3$) δ: 12.12 (s, 1H), 7.71 (m, 2H), 7.48 (m, 3H), 7.16 (t, J = 8.5 Hz, 2H), 7.09 (t, J = 8.7 Hz, 2H), 6.74 (s, 1H), 3.58 (t, J = 5.4 Hz, 1H), 2.92 (m, 2H), 2.63 (m, 1H), 2.24 (m, 1H), 1.50 (s, 3H), 1.34 (d, J = 10.4 Hz, 1H), 0.94 (s, 3H); ^{13}C NMR (100 MHz, $CDCl_3$) δ: 169.30, 165.82, 164.96, 163.53, 162.46, 161.05, 139.61, 132.47, 132.44, 131.87, 131.79, 130.25, 130.23, 129.78, 127.76, 127.68, 123.74, 123.71, 116.95, 116.73, 115.61, 115.40, 100.33, 100.32, 44.44, 42.31, 39.31, 31.60, 27.80, 26.02, 21.57. HR-MS (ESI^+): *m/z* calculated for $C_{25}H_{23}F_2N_3S$ $[M+H]^+$ 436.1659, found 436.1668.

*4.1.4.11. 4-(2-(2-(3-(4-fluorobenzylidene)-6,6-dimethylbicyclo[3.1.1] heptan-2-ylidene)hydrazinyl)thiazol-4-yl)phenol (**5k**)*. Yield 69.8%; m.p. 180–183.2 °C. ^{1}H NMR (400 MHz, C_5D_5N) *δ*: 8.10 (d, *J* = 8.6 Hz, 2H), 7.83 (s, 1H), 7.58 (dd, *J* = 5.6, 8.6 Hz, 2H), 7.24 (t, *J* = 8.6 Hz, 1H), 7.12 (s, 1H), 3.81 (t, *J* = 5.6 Hz, 1H), 2.89 (m, 1H), 2.79 (m, 1H), 2.48 (m, 1H), 2.06 (m, 1H), 1.26 (s, 3H), 1.24 (d, *J* = 2.9, 1H), 0.86 (s, 3H); ^{13}C NMR (100 MHz, C_5D_5N) *δ*: 170.76, 163.08, 160.63, 158.64, 151.78, 154.79, 134.00, 133.97, 132.23, 132.21, 131.88, 131.81, 127.75, 127.28, 125.94, 116.29, 115.61, 115.40, 100.74, 42.71, 41.05, 31.92, 28.24, 25.77, 21.34. HR-MS (ESI^+): *m/z* calculated for $C_{25}H_{24}FN_3OS$ $[M+H]^+$ 434.1702, found 434.1540.

*4.1.4.12. 2-(2-(3-(4-fluorobenzylidene)-6,6-dimethylbicyclo[3.1.1] heptan-2-ylidene)hydrazinyl)-4-(4-methoxyphenyl)thiazole (**5l**)*. Yield 81.5%; m.p. 213.6–215.7 °C. ^{1}H NMR (400 MHz, $CDCl_3$) *δ*: 12.57 (s, 1H), 7.66 (d, *J* = 8.8 Hz, 2H), 7.50 (m, 3H), 7.11 (t, *J* = 8.6 Hz, 2H), 7.00 (d, *J* = 8.9 Hz, 2H), 6.59 (s, 1H), 3.85 (s, 3H), 3.63 (t, *J* = 5.4 Hz, 1H), 2.87 (m, 2H), 2.66 (m, 1H), 2.26 (m, 1H), 1.53 (s, 3H), 1.36 (d, *J* = 10.4 Hz, 1H), 0.96 (s, 3H); ^{13}C NMR (100 MHz, $CDCl_3$) *δ*: 169.31, 165.31, 140.52, 134.73, 133.86, 131.25, 130.31, 129.55, 129.50, 128.65, 127.33, 125.55, 100.94, 44.41, 42.25, 39.26, 31.67, 27.81, 25.99, 21.57. HR-MS (ESI^+): *m/z* calculated for $C_{26}H_{26}FN_3OS$ $[M+H]^+$ 448.1859, found 448.1867.

*4.1.4.13. 2-(2-(3-(4-methoxybenzylidene)-6,6-dimethylbicyclo[3.1.1] heptan-2-ylidene)hydrazinyl)-4-phenylthiazole (**5m**)*. Yield 70.3%; m.p. 180.8–184.9 °C. ^{1}H NMR (400 MHz, $CDCl_3$) *δ*: 12.56 (s, 1H), 7.71 (d, *J* = 7.0 Hz, 2H), 7.46 (m, 6H), 6.94 (d, *J* = 8.7 Hz, 2H), 6.76 (s, 1H), 3.85 (s, 3H), 3.60 (t, *J* = 5.3 Hz, 1H), 2.93 (s, 2H), 2.63 (m, 1H), 2.24 (m, 1H), 1.51 (s, 3H), 1.35 (d, *J* = 10.3 Hz, 1H), 0.94 (s, 3H); ^{13}C NMR (100 MHz, $CDCl_3$) *δ*: 169.21, 166.14, 159.55, 140.52, 131.77, 130.60, 130.35, 129.62, 129.17, 128.37, 127.46, 125.63, 114.02, 100.69, 55.42, 44.46, 42.25, 39.47, 31.89, 27.97, 26.13, 21.65. HR-MS (ESI^+): *m/z* calculated for $C_{26}H_{27}N_3OS$ $[M+H]^+$ 430.1953, found 430.1974.

*4.1.4.14. 4-(4-fluorophenyl)-2-(2-(3-(4-methoxybenzylidene)-6,6-dimethylbicyclo[3.1.1]heptan-2-ylidene)hydrazinyl)thiazole (**5n**)*. Yield 81.5%; m.p. 180.8–184.9 °C.^{1}H NMR (400 MHz, $CDCl_3$) *δ*: 12.50 (s, 1H), 7.73 (dd, *J* = 8.8, 5.0 Hz, 2H), 7.51 (s, 1H), 7.49 (d, *J* = 8.8 Hz, 2H), 7.18 (t, *J* = 8.5 Hz, 2H), 6.95 (d, *J* = 8.7 Hz, 2H), 6.69 (s, 1H), 3.86 (s, 3H), 3.58 (t, *J* = 5.3 Hz, 1H), 2.94 (s, 2H), 2.64 (m, 1H), 2.26 (m, 1H), 1.51 (s, 3H), 1.36 (d, *J* = 10.4 Hz, 1H), 0.95 (s, 3H); ^{13}C NMR (100 MHz, $CDCl_3$) *δ*: 169.12, 166.24, 162.40, 159.51, 139.45, 131.71, 130.62, 129.06, 128.23, 127.75, 127.66, 123.80, 123.76, 116.90, 116.68, 113.96, 100.40, 100.39, 55.35, 44.36, 42.20, 39.39, 31.80, 27.89, 26.06, 21.57. HR-MS (ESI^+): *m/z* calculated for $C_{26}H_{27}N_3OS$ $[M+H]^+$ 448.1859, found 448.1860.

*4.1.4.15. 4-(2-(2-(3-(4-methoxybenzylidene)-6,6-dimethylbicyclo[3.1.1] heptan-2-ylidene)hydrazinyl)thiazol-4-yl)phenol (**5o**)*. Yield 81.5%; m.p. 205.6–207.6 °C. ^{1}H NMR (400 MHz, C_5D_5N) *δ*: 8.11 (d, *J* = 8.6 Hz, 2H), 7.94 (s, 1H), 7.63 (d, *J* = 8.7 Hz, 2H), 7.28 (d, *J* = 8.6 Hz, 2H), 7.10 (m, 3H), 3.80 (t, *J* = 5.6 Hz, 1H), 3.72 (s, 3H), 2.92 (m, 2H), 2.48 (m, 1H), 2.08 (m, 1H), 1.29 (s, 1H), 1.26 (s, 3H), 0.87 (s, 3H); ^{13}C NMR (100 MHz, C_5D_5N) *δ*: 172.28, 160.62, 160.02, 156.70, 153.28, 133.01, 131.85, 131.59, 129.20, 128.87, 128.39, 117.67, 115.71, 102.07, 56.54, 44.13, 42.45, 41.16, 33.61, 29.73, 27.25, 22.78. HR-MS (ESI^+): *m/z* calculated for $C_{26}H_{27}N_3O_2S$ $[M+H]^+$ 446.1902, found 446.1871.

*4.1.4.16. 2-(2-(3-(4-methoxybenzylidene)-6,6-dimethylbicyclo[3.1.1] heptan-2-ylidene)hydrazinyl)-4-(4-methoxyphenyl)thiazole (**5p**)*. Yield 74.4%; m.p. 193.6–196.3 °C.^{1}H NMR (400 MHz, $CDCl_3$) *δ*: 12.51 (s, 1H), 7.65 (d, *J* = 8.9 Hz, 2H), 7.50 (s, 1H), 7.49 (d, *J* = 8.9 Hz, 2H), 6.97 (dd, *J* = 15.5, 8.8 Hz, 4H), 6.57 (s, 1H), 3.85 (d, *J* = 7.0 Hz, 6H), 3.60 (t, *J* = 5.4 Hz, 1H), 2.93 (s, 2H), 2.64 (m, 1H), 2.25 (m, 1H), 1.51 (s, 3H), 1.36 (d, *J* = 10.4 Hz, 1H), 0.95 (s, 3H); ^{13}C NMR (100 MHz, $CDCl_3$) *δ*: 169.11, 165.89, 161.16, 159.54, 140.39, 131.77, 130.49, 129.22, 128.42, 127.19, 120.14, 115.01, 114.02, 98.50, 55.53, 55.43, 44.39, 42.24, 39.48, 31.91, 27.99, 26.14, 21.66. HR-MS (ESI^+): *m/z* calculated for $C_{27}H_{29}N_3O_2S$ $[M+H]^+$ 460.2059, found 460.2053.

*4.1.4.17. 2-(2-(6,6-dimethyl-3-(4-methylbenzylidene)bicyclo[3.1.1] heptan-2-ylidene)hydrazinyl)-4-phenylthiazole (**5q**)*. Yield 76.3%; m.p. 163.6–168.5 °C. ^{1}H NMR (400 MHz, $CDCl_3$) *δ*: 12.58 (s, 1H), 7.71 (d, *J* = 7.0 Hz, 2H), 7.52 (s, 1H), 7.41 (m, 5H), 7.22 (d, *J* = 7.9 Hz, 2H), 6.76 (s, 1H), 3.61 (t, *J* = 5.4 Hz, 1H), 2.94 (d, *J* = 2.8 Hz, 2H), 2.63 (m, 1H), 2.38 (s, 3H), 2.24 (m, 1H), 1.51 (s, 3H), 1.35 (d, *J* = 10.4 Hz, 1H), 0.95 (s, 3H); ^{13}C NMR (100 MHz, $CDCl_3$) *δ*: 169.35, 165.83, 140.89, 138.31, 133.64, 130.92, 130.36, 130.19, 129.79, 129.65, 129.29, 127.67, 125.69, 100.71, 44.47, 42.31, 39.48, 31.89, 27.97, 26.16, 21.69, 21.44. HR-MS (ESI^+): *m/z* calculated for $C_{26}H_{27}N_3S$ $[M+H]^+$ 414.2004, found 414.2004.

*4.1.4.18. 2-(2-(-6,6-dimethyl-3-(-4-methylbenzylidene)bicyclo[3.1.1] heptan-2-ylidene)hydrazinyl)-4-(4-fluorophenyl)thiazole (**5r**)*. Yield 79.0%; m.p. 177.0–180.8 °C. ^{1}H NMR (400 MHz, $CDCl_3$) *δ*: 7.73 (dd, *J* = 8.8, 5.0 Hz, 2H), 7.53 (s, 1H), 7.42 (d, *J* = 8.0 Hz, 2H), 7.23 (d, *J* = 7.9 Hz, 2H), 7.18 (t, *J* = 8.6 Hz, 2H), 6.70 (s, 1H), 4.94 (s, 2H), 3.57 (t, *J* = 5.4 Hz, 1H), 2.95 (s, 2H), 2.64 (m, 1H), 2.39 (s, 3H), 2.25 (m, 1H), 1.51 (s, 3H), 1.36 (d, *J* = 10.4 Hz, 1H), 0.95 (s, 3H); ^{13}C NMR (100 MHz, $CDCl_3$) *δ*: 169.24, 165.76, 164.87, 162.37, 139.87, 138.24, 133.50, 130.88, 130.10, 129.62, 129.19, 127.76, 127.68, 124.06, 124.02, 116.85, 116.63, 100.58, 100.56, 44.29, 42.21, 39.36, 31.77, 27.85, 26.04, 21.58, 21.34. HR-MS (ESI^+): *m/z* calculated for $C_{26}H_{26}FN_3S$ $[M+H]^+$ 432.1910, found 432.1917.

*4.1.4.19. 4-(2-(2-(6,6-dimethyl-3-(4-methylbenzylidene)bicyclo[3.1.1] heptan-2-ylidene)hydrazinyl)thiazol-4-yl)phenol (**5s**)*. Yield 61.0%; m.p. 159.3–161.6 °C. ^{1}H NMR (400 MHz, C_5D_5N) *δ*: 8.10 (d, *J* = 8.6 Hz, 2H), 7.94 (s, 1H), 7.57 (m, 3H), 7.28 (t, *J* = 7.9 Hz, 4H), 7.11 (s, 1H), 3.80 (t, *J* = 5.6 Hz, 1H), 2.90 (m, 2H), 2.47 (m, 1H), 2.27 (s, 3H), 2.06 (m, 1H), 1.27 (s, 4H), 1.25 (s, 4H), 0.86 (s, 3H); ^{13}C NMR (100 MHz, C_5D_5N) *δ*: 172.01, 159.81, 156.21, 153.01, 138.29, 132.71, 131.30, 130.59, 128.94, 128.40, 117.45, 101.86, 58.36, 43.88, 42.19, 40.85, 33.36, 29.46, 26.98, 22.53, 22.19. HR-MS (ESI^+): *m/z* calculated for $C_{26}H_{27}N_3OS$ $[M+H]^+$ 430.1953, found 430.1935.

*4.1.4.20. 2-(2-(6,6-dimethyl-3-(4-methylbenzylidene)bicyclo[3.1.1] heptan-2-ylidene)hydrazinyl)-4-(4-fluorophenyl)thiazole (**5t**)*. Yield 69.2%; m.p. 207.6–209.4 °C. ^{1}H NMR (400 MHz, $CDCl_3$) *δ*: 12.53 (s, 1H), 7.66 (d, *J* = 8.8 Hz, 2H), 7.53 (s, 1H), 7.43 (d, *J* = 8.0 Hz, 2H), 7.23 (d, *J* = 7.9 Hz, 2H), 7.00 (d, *J* = 8.8 Hz, 2H), 6.57 (s, 1H), 3.85 (s, 3H), 3.62 (t, *J* = 5.4 Hz, 1H), 2.96 (s, 2H), 2.65 (dt, *J* = 10.9, 5.7 Hz, 1H), 2.40 (s, 3H), 2.25 (tt, *J* = 6.0, 3.2 Hz, 1H), 1.52 (s, 3H), 1.36 (d, *J* = 10.3 Hz, 1H), 0.96 (s, 3H); ^{13}C NMR (100 MHz, $CDCl_3$) *δ*: 169.21, 165.79, 161.19, 140.48, 138.29, 133.64, 130.88, 130.19, 129.79, 129.28, 127.21, 120.15, 115.04, 98.51, 55.55, 44.45, 42.30, 39.47, 31.89, 27.96, 26.15, 21.68, 21.44. HR-MS (ESI^+): *m/z* calculated for $C_{27}H_{29}N_3OS$ $[M+H]^+$ 444.2110, found 444.2116.

*4.1.4.21. 2-(2-(3-(4-chlorobenzylidene)-6,6-dimethylbicyclo[3.1.1] heptan-2-ylidene)hydrazinyl)-4-phenylthiazole (**5u**)*. Yield 85.2%; m.p. 185.6–189.9 °C. ^{1}H NMR (400 MHz, $CDCl_3$) *δ*: 12.68 (s, 1H), 7.74 (d, *J* = 6.9 Hz, 2H), 7.58 (m, 6H), 7.12 (t, *J* = 8.7 Hz, 2H), 6.75 (s, 1H), 3.64 (t, *J* = 5.4 Hz, 1H), 2.93 (m, 2H), 2.67 (m, 1H), 2.26 (m, 1H), 1.53 (s, 3H), 1.37 (d, *J* = 10.4 Hz, 1H), 0.97 (s, 3H); ^{13}C NMR (100 MHz, $CDCl_3$) *δ*: 169.42, 165.47, 140.75, 134.84, 133.97, 131.37, 131.34, 130.45, 129.67, 129.61, 128.75, 127.45, 125.67, 100.78, 44.53, 42.36, 39.37, 31.77, 27.91, 26.09, 21.67. HR-MS (ESI^+): *m/z* calculated for $C_{25}H_{24}ClN_3S$ $[M+H]^+$ 434.1497, found 434.1538.

4.1.4.22. 2-(2-(3-(4-chlorobenzylidene)-6,6-dimethylbicyclo[3.1.1] heptan-2-ylidene)hydrazinyl)-4-(4-fluorophenyl)thiazole ***(5v)***. Yield 87.6%; m.p. 199.2–201.3 °C.^{1}H NMR (400 MHz, $CDCl_3$) δ: 12.59 (s, 1H), 7.74 (dd, J = 8.8, 5.0 Hz, 2H), 7.50 (m, 3H), 7.20 (t, J = 8.5 Hz, 2H), 7.11 (t, J = 8.6 Hz, 2H), 6.69 (s, 1H), 3.61 (t, J = 5.4 Hz, 1H), 2.93 (m, 2H), 2.66 (m, 1H), 2.27 (m, 1H), 1.53 (s, 3H), 1.37 (d, J = 10.4 Hz, 1H), 0.96 (s, 3H); ^{13}C NMR (100 MHz, $CDCl_3$) δ: 169.30, 165.82, 164.96, 163.53, 162.46, 161.05, 139.61, 132.47, 132.44, 131.87, 131.79, 130.25, 130.23, 129.78, 127.76, 127.68, 123.74, 123.71, 116.95, 116.73, 115.61, 115.40, 100.33, 100.32, 44.44, 42.31, 39.31, 31.60, 27.80, 26.02, 21.57. HR-MS (ESI^+): *m/z* calculated for $C_{25}H_{23}ClFN_3S$ $[M+H]^+$ 452.1363, found 418.1753.

4.1.4.23. 4-(2-(2-(3-(4-chlorobenzylidene)-6,6-dimethylbicyclo[3.1.1] heptan-2-ylidene)hydrazinyl)thiazol-4-yl)phenol ***(5w)***. Yield 62.3%; m.p. 205.6–207.3 °C.^{1}H NMR (400 MHz, C_5D_5N) δ: 8.11 (d, J = 8.7 Hz, 2H), 7.82 (s, 1H), 0.85 (s, 3H), 7.54 (d, J = 8.7 Hz, 2H), 7.48 (d, J = 8.6 Hz, 2H), 7.28 (d, J = 8.7 Hz, 2H), 7.12 (s, 1H), 3.80 (t, J = 5.6 Hz, 1H), 2.89 (dd, J = 2.4, 17.1 Hz, 1H), 2.79 (m, 1H), 2.48 (m, 1H), 2.06 (m, 1H), 1.25 (s, 3H), 1.24 (s, 1H), 0.87 (s, 3H); ^{13}C NMR (100 MHz, C_5D_5N) δ: 172.14, 160.11, 155.88, 153.26, 137.73, 134.75, 134.03, 132.87, 130.16, 129.21, 128.77, 127.17, 117.71, 102.19, 44.12, 42.45, 41.02, 33.44, 29.70, 27.18, 22.76. HR-MS (ESI^+): *m/z* calculated for $C_{25}H_{24}ClN_3OS$ $[M+H]^+$ 450.1407, found 450.1370.

4.1.4.24. 2-(2-(3-(4-chlorobenzylidene)-6,6-dimethylbicyclo[3.1.1] heptan-2-ylidene)hydrazinyl)-4-(4-methoxyphenyl)thiazole ***(5x)***. Yield 76.1%; m.p. 205.6–207.3 °C.^{1}H NMR (400 MHz, C_5D_5N) δ: 8.08 (d, J = 8.8 Hz, 2H), 7.81 (s, 1H), 7.54 (d, J = 8.6 Hz, 2H), 7.48 (d, J = 8.6 Hz, 2H), 7.17 (s, 1H), 7.04 (d, J = 8.8 Hz, 2H), 3.81 (t, J = 5.6 Hz, 1H), 3.68 (s, 3H), 2.88 (m, 1H), 2.80 (m, 1H), 2.48 (m, 1H), 2.06 (m, 1H), 1.26 (s, 3H), 1.23 (s, 1H), 0.85 (s, 3H); ^{13}C NMR (100 MHz, C_5D_5N) δ: 172.20, 160.96, 156.02, 152.80, 137.68, 134.72, 134.04, 132.87, 130.17, 130.14, 128.92, 127.21, 115.74, 103.10, 56.53, 44.15, 42.46, 41.01, 33.44, 29.70, 27.19, 22.78. HR-MS (ESI^+): *m/z* calculated for $C_{26}H_{26}ClN_3OS$ $[M+H]^+$ 464.1563, found 464.1581.

4.2. Biology

4.2.1. MTT activity

Three cancer cell lines (Hela, SM7721, and CT-26 cells) were incubated in DMEM and RPMI-1640 medium (Gibco, Milano, Italy) containing 10% FBS at 37 °C in a 5% CO_2 humidified incubator. Cells were grown in 96-well plates at a density of 5×10^3 cells/well and incubated overnight at 37 °C, 5% CO_2. compounds **5a–5g** were dissolved to 10 mM DMSO and diluted in serum free medium to the final concentrations. After treatment with different concentrations of compounds for 72 h, a volume of 10 μL MTT solution was added to each well and cells were incubated for 4 h. Subsequently, the solution was removed and formazan crystals were dissolved in 100 μL of DMSO. Absorbance was measured at 540 nm wavelength using a microplate.

4.2.2. Cell apoptosis analysis

Hela cells were seeded at 2×10^5/wells and incubated overnight at 37 °C, 5% CO_2. The compounds were dissolved DMSO to 10 mM, and diluted in DMEM medium to the needed concentrations (2.5, 5, or 10 μM). After treatment with different concentrations of compound **5g** for 72 h, cells were harvested and washed twice with cold phosphate-buffered saline (PBS). Then, cells were stained with Annexin V-APC/PI solution at room temperature for 15 min in the dark. Finally, stained cells were analyzed for apoptosis using flow cytometry (BD Accuri C6).

4.2.3. Cell cycle analysis

For flow cytometric analysis of DNA content, 5×10^5 Hela cells were seeded in six well plates. After overnight incubation at 37 °C, cells were treated with different concentrations of compounds **5g** (2.5, 5, or 10 μM) for 72 h. Then, cells were collected, centrifuged, and fixed overnight with ice cold ethanol (70%) at −20 °C. Then, cells were treated with 100 μg/mL RNase A buffer for 30 min and stained with PI in the dark at 4 °C for 30 min. Finally, samples were analyzed for DNA content by flow cytometry (BD FACS Canto II).

4.2.4. Mitochondrial membrane potential assay

Hela cells were treated with different concentration of compound **5g** for 72 h in 6-well plates. Then, cells were washed with cold PBS and incubated with 1 μg/mL of JC-1 (5,5′,6,6′-tetrachloro-1,1′,3,3′-tetrethylbenzimidalylcarbocyanineiodide) working solution in culture medium without FBS for 20 min at 37 °C in the dark. The red/green fluorescence intensity was determined by flow cytometry (Becton-Dickinson FACS Calibur).

4.2.5. Analysis of reactive oxygen species

After treatment of 1×10^6 Hela cells with compound **5g** (2.5, 5, or 10 μM) in 6-well plates for 72 h, the medium was discarded and cells were washed twice with PBS. Then, fresh FBS-free medium, containing ROS indicator 2′,7′-dichlorodihydrofluorescein diacetate (DCFH-DA, 10 μM) was added to each well and cells were incubated for 20–30 min at 37 °C in the dark. Next, cells were visualized and imaged under an inverted fluorescence microscopy. For intracellular ROS analysis, treated cells were collected by trypsinization and centrifugation, washed with PBS, and stained with Carboxy-DCFDA (10 μM). The DCF fluorescent intensity was determined by flow cytometry (Becton-Dickinson FACS Calibur).

4.2.6. Western blot analysis

For Western blot analysis, Hela cells (1×10^6 cells/ml) were treated with 0, 5, and 10 μM of compound **5g** for 72 h. After treatment, cells were washed twice with PBS, 200 μL of lysis buffer was added, and cells were resuspended. The lysate was centrifuged at 13000 rpm for 10 min at 4 °C. Then, supernatants were collected and the protein concentrations were determined using a BCA Protein Assay Kit (KeyGEN Biotech., China). Equal amounts of protein (50 μg) were separated by electrophoresis using a 12% SDS–PAGE gel and transferred to a nitrocellulose membrane (Millipore, Billerica, MA, USA). Membranes were blocked with 5% nonfat milk in Tris-buffered saline, containing 0.1% Tween-20 (TBST) at room temperature for 1 h, washed three times with TBST and incubated overnight with monocloonal primary antibodies from Cell Signaling Technology (Beverly, MA, USA) at 4 °C. After being washed three times with TBST, membranes were incubated with anti-mouse or anti-rabbit horseradish peroxidase (HRP)-conjugated secondary antibodies (1:5000) for 2 h at room temperature and blocked with 5% nonfat milk in TBST. To visualize proteins, membranes were washed three times with TBST and exposed to an enhanced chemiluminescence (ECL) detection reagent. BioMax film was used for Western blot analysis. Blots were quantified by laser scanning densitometry.

Conflict of interest

The authors declare no conflict of interest.

Acknowledgements

This study was supported by the National Natural Science Foundation of China (No. 31470592), Jiangsu Provincial Key Lab for the Chemistry and Utilization of Agro-Forest Biomass, and the Priority

Academic Program Development of Jiangsu Higher Education Institutions (Jiangsu, China).

Appendix A. Supplementary material

Supplementary data to this article can be found online at https://doi.org/10.1016/j.bioorg.2018.12.010.

References

[1] P.D. Ray, B.W. Huang, Y. Tsuji, Cell Signal 24 (2012) 981–990.
[2] H.U. Simon, A. Hajyehia, F. Levischaffer, Apoptosis 5 (2000) 415–418.
[3] G.C. Brown, V. Borutaite, Mitochondrion 12 (2012) 1–4.
[4] S. Wang, Y. Wang, X. Liu, et al., J. Ethnopharmacol. 187 (2016) 42–48.
[5] S. Elmore, Toxicol. Pathol. 35 (2007) 495–516.
[6] M.O. Hengartner, H.R. Horvitz, Philos. Trans. R Soc. Lond. B Biol. Sci. 345 (1994) 243–246.
[7] J. Yang, X. Liu, K. Bhalla, et al., Science 275 (1997) 1129–1132.
[8] S. Manon, B. Chaudhuri, M. Guérin, Febs Lett. 415 (1997) 29–32.
[9] B. Antonsson, S. Montessuit, B. Sanchez, et al., J. Biol. Chem. 276 (2001) 11615–11623.
[10] Q. Hou, E. Cymbalyuk, S.C. Hsu, et al., Apoptosis 8 (2003) 617–629.
[11] P. Li, D. Nijhawan, I. Budihardjo, et al., Cell 91 (1997) 479–489.
[12] M.V. Sobral, A.L. Xavier, T.C. Lima, et al., Sci. World J. 2014 (2014) 953451.
[13] A.B. Oskuie, S.A. Nasrollahi, S. Nafisi, J. Drug. Deliv. Sci. Tecnol. 43 (2018) 327–332.
[14] W. Chen, Y. Liu, M. Li, et al., J. Pharmacol. Sci. 127 (2015) 332–338.
[15] A.M. Leite, E.D.O. Lima, E.L.D. Souza, et al., Braz J. Pharm. Sci. 43 (2007) 121–126.
[16] H. Kasuya, S. Iida, K. Ono, et al., Nat. Prod. Commun. 10 (2015) 1479–1482.
[17] S. Liao, S. Shang, M. Shen, et al., Bioorg. Med. Chem. Lett. 26 (2016) 1512–1515.
[18] D.H. Vyas, S.D. Tala, J.D. Akbari, et al., Indian J. Chem. B 48 (2009) 833–839.
[19] E.S. Ibrahim, G.E.H. Elgemeie, M.M. Abbasi, et al., Nucleos. Nucleot. Nucl. 14 (1995) 1415–1423.
[20] S.V. Kiselev, L.E. Nikitina, V.A. Startseva, et al., Pharm. Chem. J. 51 (2017) 343.
[21] S.B. Bharate, S.I. Khan, B.L. Tekwani, et al., Bioorg. Med. Chem. 16 (2008) 1328–1336.
[22] N.K. Sahu, S.S. Balbhadra, J. Choudgary, et al., Curr. Med. Chem. 19 (2012) 209–225.
[23] S.N. Bukhari, I. Jantan, O. Unsal Tan, M. Sher, et al., J. Agric. Food Chem. 62 (2014) 5538–5547.
[24] D. Maydt, S. De Spirt, C. Muscgelknautz, et al., Xenobiotica 43 (2013) 711–718.
[25] H.N. Pati, U. Das, R.K. Sharma, et al., Mini Rev. Med. Chem. 7 (2007) 131–139.
[26] C.M.D. Silva, D.L.D. Silva, L.V. Modolo, et al., J. Adv. Res. 2 (2011) 1–8.
[27] D.J. Hadjipavlou-Litina, A.A. Geronikaki, Drug Des. Discov. 15 (1998) 199–206.
[28] A.A. Shaikh, M.G. Raghuwanshi, K.I. Molvi, et al., J. Chem. Pharm. Res. 5 (2013) 14–25.
[29] Z. Xu, J. Guo, Y. Yang, et al., Eur. J. Med. Chem. 123 (2016) 309–316.
[30] J.R. Li, D.D. Li, R.R. Wang, et al., Eur. J. Med. Chem. 75 (2014) 438–447.
[31] H.N. Karade, A.M. Sathe, M.P. Kaushik, Med. Chem. Res. 17 (2008) 19–29.
[32] R.G. Kalkhambkar, G.M. Kulkami, H. Shivkumar, et al., Eur. J. Med. Chem. 42 (2007) 1272–1276.
[33] T.I. de Santana, M.O. Barbosa, A.C.N. da Cruz, et al., Eur. J. Med. Chem. 144 (2017) 874–886.
[34] W. Xie, Y. Wu, J. Zhang, et al., Eur. J. Med. Chem. 145 (2018) 35–40.
[35] M.S. Al-Said, M.S. Bashandy, S.I. Al-Qasoumi, et al., Eur. J. Med. Chem. 46 (2011) 137–141.
[36] K. Ahmed, Y. Matsuya, H. Nemoto, et al., Chem.-Biol. Interact. 177 (2009) 218–226.
[37] M. Juneja, U. Vanam, S. Paranthaman, et al., Eur. J. Med. Chem. 63 (2013) 474–483.
[38] M.K. Bao, S.S. Xiong, M.Z. Cao, et al., Chin. J. Org. Chem. 34 (2014) 2130–2134, https://doi.org/10.6023/cjoc201404021.
[39] J. Rui, J.L. Yang, J.F. Hang, et al., Chin. J. Org. Chem. 36 (2016) 2183–2190, https://doi.org/10.6023/cjoc201603023.
[40] M.K. Bao, Y.Q. Yang, W. Gu, et al., Chin. J. Org. Chem. 34 (2014) 2146–2151, https://doi.org/10.6023/cjoc201404049.
[41] N. Sun, X. Wang, Z.B. Ding, et al., Chin. J. Org. Chem. 36 (2016) 2489–2495, https://doi.org/10.6023/cjoc201604042.
[42] J.L. Yang, J. Rui, X. Xu, et al., RSC Adv. 6 (2016) 111760–111766.
[43] J.L. Yang, H.J. Xu, X. Xu, et al., Dyes Pigments. 128 (2016) 75–83.
[44] Y.Y. Wang, W. Gu, Y. Shan, et al., Bioorg. Med. Chem. Lett. 27 (2017) 2360–2363.
[45] G. Szilágyi, L. Simon, P. Koska, et al., Neurosci. Lett. 399 (2006) 206–209.
[46] S. Gupta, G.E. Kass, E. Szegezdi, et al., J. Cell. Mol. Med. 13 (2009) 1004–1033.
[47] X.D. Wang, Genes Dev. 15 (2001) 2922–2933.
[48] B. Liu, W.W. Ao, Y. Yang, et al., J. Nanjing Forest. Univ. (Nat. Sci. Ed). 02 (2010) 89–94.